

1 **Ice-cored moraine degradation mapped and quantified using an**
2 **unmanned aerial vehicle: a case study from a polythermal glacier**
3 **in Svalbard**

4 Tonkin, T.N^{a,*}, Midgley, N.G^a, Cook, S.J^b and Graham, D.J^c

5

6 ^a School of Animal, Rural and Environmental Sciences, Nottingham Trent
7 University, Brackenhurst Campus, Southwell, Nottinghamshire, UK

8

9 ^b School of Science and the Environment, Manchester Metropolitan
10 University, Manchester, UK

11

12 ^c Polar and Alpine Research Centre, Department of Geography,
13 Loughborough University, Leicestershire, UK

14

15 * Corresponding Author: + 44 115 848 5257 toby.tonkin@ntu.ac.uk

16

17 **Keywords**

18

19 Structure-from-Motion, deglaciation, geomorphologic change detection,
20 Austre Lovénbreen

21 **Highlights**

- 22 · SfM photogrammetry used to produce topographic data from archive
23 aerial imagery and UAV derived aerial imagery
- 24 · Datasets from 2003 and 2014 were compared to report on the de-
25 icing of a lateral-frontal ice-cored moraine
- 26 · The moraine appears to be de-icing predominantly via down-wastage
27 affording the moraine a higher degree of stability
- 28 · UAVs and SfM are shown to be useful tools for monitoring
29 environmental change

30 **Abstract**

31 Ice-cored lateral-frontal moraines are common at the margins of receding
32 high-Arctic valley glaciers, but the preservation potential of these features
33 within the landform record is unclear. Recent climatic amelioration provides
34 an opportunity to study the morphological evolution of these landforms as
35 they de-ice. This is important because high-Arctic glacial landsystems have
36 been used as analogues for formerly glaciated areas in the mid-latitudes.
37 This study uses SfM (Structure-from-Motion) photogrammetry and a
38 combination of archive aerial and UAV (unmanned aerial vehicle) derived
39 imagery to investigate the degradation of an ice-cored lateral-frontal
40 moraine at Austre Lovénbreen, Svalbard. Across the study area as a whole,
41 over an 11-year period, the average depth of surface lowering was $-1.75 \pm$
42 0.89 m. The frontal sections of the moraine showed low or undetectable
43 rates of change. Spatially variable rates of surface lowering are associated

44 with differences in the quantity of buried ice within the structure of the
45 moraine. Morphological change was dominated by surface lowering, with
46 limited field evidence of degradation via back-wastage. This permits the
47 moraine a greater degree of stability than observed at other sites in
48 Svalbard. It is unclear whether the end point will be a fully stabilised ice-
49 cored moraine, in equilibrium with its environment, or an ice-free lateral-
50 frontal moraine complex. Controls on geomorphological change (e.g.
51 topography and climate) and the preservation potential of the lateral-
52 frontal moraine are discussed. The methods used by this research also
53 demonstrate the potential value of SfM photogrammetry and unmanned
54 aerial vehicles for monitoring environmental change and are likely to have
55 wider applications in other geoscientific sub-disciplines.

56 **1. Introduction**

57 In Svalbard, the Neoglacial maxima of land-terminating glaciers are
58 typically demarcated by large lateral-frontal moraine complexes (e.g.
59 Bennett et al., 1996; Lyså and Lønne, 2001; Glasser and Hambrey, 2003;
60 Lønne and Lyså, 2005; Lukas et al. 2005; Ewertowski et al. 2012; Midgley
61 et al., 2013). The persistence of relict ice in such moraines is testament to
62 extensive permafrost conditions at the margins of these glaciers
63 (Etzelmüller and Hagen, 2005). However, climatic amelioration and
64 deglaciation are contributing to the de-icing of ice-cored landforms (e.g.
65 Etzelmüller, 2000). Whilst the dynamics of de-icing have been studied (e.g.
66 Schomacker 2008; Irvine-Fynn et al., 2011; Bennett and Evans, 2012), the

67 resulting preservation potential of these landforms in the geomorphological
68 record is unclear (Bennett et al., 2000; Evans, 2009). Knowledge regarding
69 the formation and preservation of glacial landforms is of interest due to the
70 potential for contemporary glacial environments to be used as analogues
71 for formerly glaciated environments in the mid-latitudes (e.g. Hambrey et
72 al., 1997; Graham and Midgley, 2000; Benn and Lukas, 2006; Graham and
73 Hambrey, 2007; Midgley et al., 2007). Moraines are important
74 palaeoenvironmental proxies (Kirkbride and Winkler, 2012), and
75 understanding their genesis and potential for preservation in the
76 geomorphological record is an essential prerequisite for robust
77 interpretations of relict moraine assemblages. Rates of wastage on ice-
78 cored moraines are understood to be principally driven by surface processes
79 and topography, rather than climatic conditions (Schomacker, 2008). In
80 the high-Arctic glacial environment, some ice-cored moraines are reported
81 to be unstable and somewhat transient geomorphological features, with
82 ultimately low preservation potential (Bennett et al., 2000; Lukas et al.,
83 2005). Conversely, where debris cover is sufficiently thick, it has been
84 reported that ice-cored moraine may stabilise, undergoing limited or
85 negligible rates of transformation (Ewertowski, 2014; Ewertowski and
86 Tomczyk, 2015).

87 Geoscientists now have access to a range of new technologies for
88 monitoring the temporal evolution of geomorphological systems.
89 Specifically, automated photogrammetric techniques such as SfM are an
90 excellent tool for conducting high-resolution topographic surveys (James

91 and Robson, 2012; Westoby et al., 2012; Carrivick et al., 2013; Fonstad et
92 al., 2013). SfM photogrammetry has also been integrated with small format,
93 low-level aerial imagery acquired from small UAVs (e.g. Lucieer et al., 2013;
94 Tonkin et al., 2014; Ryan et al., 2015; Smith and Vericat, 2015; Clapyut
95 et al., 2015; Rippin et al., 2015). Here, SfM photogrammetry was used to
96 document the evolution of an ice-cored lateral-frontal moraine over an 11-
97 year study period, based on images obtained with a UAV in 2014 and
98 archive images from a piloted aircraft in 2003. The principal aims of this
99 study were to: (1) report on the use of SfM for Digital Elevation Model (DEM)
100 production from both archive and small-format low-level aerial imagery for
101 the purpose of assessing environmental change in the high-Arctic; (2)
102 investigate landform evolution at the margins of a high-Arctic glacier; and
103 (3) discuss the geomorphological evolution of ice-cored moraine in relation
104 to landform stability and preservation potential.

105 **2. Study site**

106 Austre Lovénbreen is a c. 5 km long valley glacier located on
107 Brøggerhalvøya, Spitsbergen, Svalbard (78°53'12"N 12°08'50"E; Fig. 1).
108 The thermal regime of the glacier was polythermal in 2010 based on our
109 interpretation of GPR (ground-penetrating radar) profiles presented by
110 Saintenoy et al. (2012); the extent of temperate ice appeared to be
111 exceptionally spatially limited, with the glacier being almost entirely cold-
112 based. Austre Lovénbreen has a strong negative mass balance according
113 to Friedt et al. (2012), who reported a mean ablation rate of 0.43 m a⁻¹

114 between 1962 and 1995, which increased to 0.70 m a⁻¹ for the 1995–2009
115 period.

116 The glacier is surrounded by mountainous terrain with peaks ranging from
117 583 m a.s.l. (Slattofjellet) to 879 m a.s.l. (Nobilefjellet) at the head of the
118 basin. Surge-type glacier behaviour is widely reported in Svalbard (e.g.
119 Jiskoot et al., 2000). The potential for surge-type behaviour at adjacent
120 glaciers on Brøggerhalvøya has been discussed (e.g. Hansen, 2003; Glasser
121 et al., 2004; Hambrey et al., 2005) and disputed (e.g. Jiskoot et al., 2000;
122 King et al., 2008). However, Midgley et al. (2013) presented evidence that
123 Austre Lovénbreen may have surged close to or at its Neoglacial maximum
124 position based upon the interpretation of oblique Norsk Polarinstitut (NPI)
125 aerial imagery from 1936.

126 The character of the glacier forefield was documented by Hambrey et al.
127 (1997), with additional field observations reported by Graham (2002). The
128 glacier forefield is characterised by a large arcuate lateral-frontal moraine,
129 which is breached at two locations by the main contemporary glaciofluvial
130 outlets. The lateral-frontal moraine demarcates the Neoglacial limit based
131 upon interpretation of ground-level imagery from 1907 (Isachsen, 1912)
132 and oblique Norsk Polarinstitut (NPI) aerial images from 1936 (Fig. 6 in
133 Midgley et al., 2013). The glacier has receded c. 1 km from this position.
134 Within the Neoglacial limit, surface hummocks ('hummocky moraine') are
135 identified. Fluted diamicton plains and lineated accumulations of
136 supraglacial debris (e.g. Hambrey et al., 1997) have developed as Austre

137 Lovénbreen receded from its Neoglacial position. More recently, the
138 structural characteristics of the lateral-frontal moraine around the western
139 margin of the forefield were investigated by Midgley et al. (2013) using
140 GPR. This research found that in lateral sections an ice-core constitutes a
141 significant component of the landform, in contrast to the frontal sections
142 where the occurrence of buried ice is limited. This paper maintains the focus
143 on the western margin of the forefield, providing surface morphological
144 data to complement the subsurface data presented by Midgley et al. (2013).

145 **3. Materials and methods**

146 *3.1. Data acquisition*

147 Five images from 2003 were obtained from the UK Natural Environment
148 Research Council (NERC) Airborne Research and Survey Facility (ARSF) for
149 DEM production. These images were collected on August 9th 2003 using a
150 metric camera mounted in a Dornier 228 aircraft, and the contact prints
151 scanned to give an approximate ground resolution of 0.2 m per pixel. In
152 2014, 10 UAV sorties were flown over a two-day survey period (15th and
153 16th July 2014). The total area covered by this survey is c. 676,000 m². A
154 DJI S800 multi-rotor UAV equipped with an 18 MP Canon EOS-M consumer-
155 grade digital camera was used for image acquisition. The UAV was flown at
156 approximately 100 m above ground level, giving a ground resolution of
157 0.02 m per pixel. A total of 1856 images from this survey were used for
158 DEM production. Further details on this survey setup and validation against
159 a total station derived survey were documented by Tonkin et al. (2014).

160 Ground control points were surveyed using a Leica 1200 dGPS and post-
161 processed using RiNEX data obtained from the EUREF Permanent Network
162 station at Ny-Ålesund (http://www.epncb.oma.be/_networkdata/). For the
163 2003 imagery, three ground control points were used to georeference the
164 point cloud, and to project it to the UTM 33N coordinate system (Fig. 2).
165 These were the tops of boulders which were visible on the original scanned
166 contact prints, and also readily identified in the field. As the parts of the
167 glacier forefield are likely to be geomorphologically unstable (e.g. Irvine-
168 Fynn et al., 2011), where possible control points were located outside of
169 the Neoglacial moraine. The 2014 imagery was georeferenced using 27
170 ground control-points consisting of A3 sized paper targets placed on snow-
171 free areas of the moraine (Fig. 2).

172 *3.2. DEM generation*

173 DEM generation was conducted in Agisoft Photoscan (v. 1.1.5), a
174 commercial SfM software package. A total of 2035 tie-points were
175 automatically identified on the five images from 2003. For the 2014
176 imagery, processing was split between two 'chunks' that were merged to
177 form a single DEM of the lateral-frontal moraine. Photoscan identified a
178 total of 5,660,015 tie points from the 1856 images with the resulting DEM
179 produced from a dense point cloud of 106,484,427 points. Both SfM DEMs
180 were produced at 0.5 m per pixel resolution to facilitate comparison
181 between them. On the 2003 DEM, moraine distal slopes were subject to

182 shading, resulting in excessively interpolated elevation data. Zones
183 identified with these issues were removed prior to analysis.

184 3.3. Evaluation of DEM quality

185 LiDAR data, obtained concurrently with the 2003 aerial imagery were used
186 to independently validate the 2003 DEM. DEM elevations were compared
187 with LiDAR spot heights distributed across the area of interest, giving a
188 vertical *RMSE* (root mean square error) value of 0.888 m ($n = 768,296$; σ
189 = 0.812 m). The residuals appear to be spatially distributed and increase
190 in areas subject to poor ground control, thus the 2003 SfM DEM may
191 represent an overestimate of the surface topography. However, it is worth
192 noting that the LiDAR data are not error free – the heights have been shown
193 to have an *RMSE* value of < 0.15 m in the area of interest (Arnold et al.,
194 2006) – but as the two datasets were obtained simultaneously their
195 comparison provides an independent means of estimating DEM error.

196 Two interrelated issues are likely to account for the vertical *RMSE* value in
197 this model: (1) the use of relatively low resolution of the imagery on which
198 the DEM is based; and (2) the identification of appropriate 'stable' features
199 to use as ground-control. The first issue reduces the accuracy with which
200 the location of control points can be identified in the imagery. In practice,
201 it is estimated that the identification of control points in the images
202 introduced an error of approximately 1 m. The low resolution also meant
203 that only a small number of large boulders were visible in the imagery,
204 limiting the number of sites available for use as ground control points. This

205 issue was confounded by the need to locate control points on features that
206 were unlikely to have moved during the 11 years between image capture
207 and the field survey. Use of existing 'stable' features for ground control is
208 a limitation of studies that use photogrammetric methods to produce DEMs
209 of changing geomorphological systems (e.g. Schiefer and Gilbert, 2007;
210 Staines et al., 2015), and means it is rarely possible to achieve an optimal
211 distribution of GCPs (ground control points). In this study only three
212 suitable boulders were identified for use as GCPs, which is highly likely to
213 have contributed to an increase in errors (e.g. Clapuyt et al., 2015).

214 For the 2014 DEM, errors were calculated for 12 dGPS surveyed check
215 points, which were paper targets visible in the imagery, additional to the
216 27 control points used to generate the model (Fig. 2). Sub-decimetre
217 vertical errors were obtained for these points ($RMSE = 0.048$ m; $n = 12$).
218 These error estimates give us confidence that the DEM provides an
219 excellent representation of the moraine morphology. For additional
220 validation, randomly generated spot heights ($n = 4370$) from more
221 geomorphologically 'stable' areas (e.g. Staines et al., 2015) outside the
222 Neoglacial limit on the 2003 and 2014 SfM DEMs were compared. Values
223 from these areas show lower error levels ($RMSE = 0.374$ m; $\sigma = 0.274$ m),
224 giving confidence in the validity of the two SfM DEMs.

225 *3.4. DEM differencing and minimum levels of detection*

226 DEM differencing – subtracting spatially coincident raster grid cells from
227 each other – was used to assess the amount of morphological change

228 between 2003 and 2014. DEM differencing was conducted using the GCD
229 (Geomorphologic Change Detection, ver. 6) plugin of Wheaton et al. (2010)
230 in ArcGIS 10.2.1. The GCD plugin allows for robust error assessment
231 through the use of 'minimum levels of detection' (minLOD). This approach
232 minimises the likelihood of making spurious interpretations of apparent
233 morphological differences that are actually associated with uncertainty in
234 the data. Minimum levels of detection were calculated using a propagated
235 error value derived from error assessments undertaken on both
236 topographic surfaces (e.g. Braslington et al., 2003). The technique
237 assumes error within topographic datasets are spatially uniform, and
238 discards changes below this threshold. For the 2003–2014 time period,
239 vertical differences under 0.89 m were regarded as potentially erroneous,
240 and therefore disregarded for the purposes of assessing morphological
241 change. The majority of this uncertainty results from errors in the 2003
242 DEM. Three zones (Z_1 , Z_2 and Z_3) were clipped from the differenced DEM
243 and used to report on spatial variations in geomorphological change across
244 the landform (Fig. 3A).

245 *3.5. Feature mapping*

246 The relative abundance of features indicative of ice-cored moraine
247 degradation were mapped and used to validate the reported rates of
248 surface change derived from the DEM differencing. Features were identified
249 and mapped from ultra-high resolution (2 cm per pixel) orthorectified
250 imagery produced from the 2014 survey data. These observations were

251 supplemented by field observations collected simultaneously to the
252 acquisition of the 2014 topographic data. The study area was split into 50
253 x 50 m grid squares ($n = 234$) to allow the relative abundance of
254 geomorphological features indicative of surface change to be qualitatively
255 assessed across the study area. As the precise mode of formation for micro-
256 topographic features indicating landform degradation was unclear, we
257 adopted the non-genetic classification of 'surface linear undulations' to refer
258 to features developed by the slumping and/or the extensional surface
259 fracturing of materials in response to surface lowering (e.g. Kjær and
260 Krüger, 2001; Krüger et al., 2010). The location of a large-scale arcuate
261 edge and a linear back-wasting edge were also mapped.

262 **4. Results**

263 *4.1. DEM differencing*

264 A total area of 461,429 m² was assessed for surface elevation change (Fig.
265 3A). The lateral-frontal moraine shows a level of geomorphological stability,
266 with change detected on 52% (238,476 m²) of the study area. Ninety-six
267 percent of the area where change was detected was associated with surface
268 lowering. The total volume difference for the study area was $-377,490 \pm$
269 201,292 m³.

270 A clear spatial trend characterises the pattern of morphological change. The
271 lateral up-glacier sections are subject to higher rates of surface lowering.
272 Average surface change in Z_1 was -2.56 m for the study period. Nearly all
273 grid cells in this area were observed outside the minimum level of detection.

274 Z_2 and Z_3 , which are located in more frontal positions show diminishing
275 rates of detectable change (92.3% and 19.9% of each study area,
276 respectively) and lower rates of average net surface change (-1.49 and
277 -0.52 m, respectively). Profiles 1, 2 and 3 in Fig. 4 also demonstrate
278 reduced surface lowering in frontal positions. On profile 1, surface lowering
279 is clearly evident on the moraine ridge crest, and less extensively on the
280 ice-proximal and distal slopes. Profiles 2 and 3 show limited
281 geomorphological change with a significant proportion of change falling
282 close to or below the minLOD (Fig. 4). Detectable change on the outwash-
283 plain was limited. Areas of deposition principally occur on moraine distal
284 slopes and in proximity to glaciofluvial drainage systems. Areas that have
285 experienced deposition across the study averaged a depth of 1.42 ± 0.89 m.
286 However the deposition was extremely spatially and volumetrically limited,
287 only accounting for the movement of $17,952 \pm 11,267$ m³ of material (4%
288 of the area of detectable change) opposed to $413,394 \pm 212,243$ m³ of
289 change associated with surface lowering across the study area (Fig. 3B). It
290 should be noted that in 2014 c. 11% of the study area was covered by
291 exceptionally late-lying snow, which was typically located in sheltered areas
292 between pronounced ridges and contributes to the lowering of estimates of
293 surface change over the study period.

294 4.2. *Geomorphological evidence of surface change*

295 The occurrence of features indicative of surface evolution were mapped to
296 validate the derived rates of surface change (Fig. 5). Mapped surface

297 features indicative of surface change were identified in the lateral-zone of
298 the moraine complex; however, the features were less readily identified on
299 the frontal zone of the landform. Out of the 234 survey grid squares
300 assessed, 150 (64%) had no observable evidence of surface evolution. One
301 ice-free actively back-wasting slope was located on the frontal zone of the
302 analysis area adjacent to the western fluvial outlet channel which dissects
303 the Neoglacial lateral-frontal moraine. An additional inactive arcuate back-
304 wasting edge was identified in the lateral zone of the landform (Fig. 5). The
305 spatial occurrence of evidence associated with surface change gives us
306 confidence in the results of the DEM differencing.

307 **5. Discussion**

308 *5.1. Comparisons with other glaciers*

309 A range of studies provide rates of ice-cored landform degradation. Here,
310 rates of landform degradation appear to be limited in comparison to some
311 sites in Svalbard and elsewhere. For example, Irvine-Fynn et al. (2011)
312 report a moraine surface lowering rate of $-0.65 \pm 0.2 \text{ m a}^{-1}$ at neighbouring
313 Midtre Lovénbreen between 2003 and 2005. Longer-term changes (1984–
314 2004) at Holmstrombreen (Svalbard) were reported to have occurred at a
315 rate of -0.9 m a^{-1} (Schomacker and Kjær, 2008). Rates of surface lowering
316 in temperate Icelandic glacial environments are variable (between -0.015
317 and -1.4 m a^{-1} ; e.g. Krüger and Kjær, 2000; Schomacker and Kjær, 2007;
318 Bennett and Evans, 2012). On average, surface lowering for the entire
319 study area was considerably lower at -0.16 m a^{-1} than reported at some

320 sites in Svalbard. It should be noted that the rate of change may not have
321 remained consistent throughout the study period with moraines known to
322 be subject to short-term changes over consecutive years (e.g. Ewertowski
323 and Tomczyk, 2015). Even in areas with the highest levels of surface
324 lowering (e.g. Z₁), only modest rates of average surface change per year
325 were detected (-0.23 m a^{-1}), which at worst, can be considered an
326 overestimate of surface change, for example, due to errors on the 2003
327 SfM DEM. These results are similar to the findings of Ewertowski and
328 Tomczyk (2015) who report on surface lowering at the margins of
329 Ebbabreen and Ragnarbreen in Petuniabukta. Here, whilst areas of back-
330 wasting ice were quantified to undergo changes of up to 1.8 m a^{-1} , lower
331 levels of transformation (e.g. below 0.3 m a^{-1}), were quantified,
332 highlighting the relative stability of some ice-cored moraine in Svalbard.
333 Similarly, at Austre Lovénbreen, just over half of the study area (52%) was
334 below the minimum level of detection implying no or exceptionally limited
335 geomorphological change between 2003 and 2014.

336 *5.2. Moraine preservation potential*

337 Moraines in the high-Arctic glacial environment are understood to be highly
338 vulnerable to thermo-erosion and mass movement facilitated by fluvial
339 undercutting. This can result in high rates of landform transformation
340 (Ewertowski and Tomczyk, 2015). The evidence presented here indicates
341 that such surface processes are less important with regard to the
342 transformation of the lateral-frontal moraine at Austre Lovénbreen. A

343 surface excavation in proximity to Z_1 showed that the debris mantle was
344 surprisingly thick at 1.6 m. At this site, and potentially others, whilst rates
345 of moraine surface lowering may be rather high, a relatively thick and
346 evenly distributed debris-layers can permit the relative stabilisation of ice-
347 cored moraine where the coupling of slope and fluvial processes (e.g.
348 Etzelmüller et al., 2000) exert less influence on moraine transformation.
349 This is largely due to the less topographically confined setting of the lateral-
350 frontal complex at Austre Lovénbreen, which results in the glaciofluvial
351 system being well separated from the moraine. The result is a low level of
352 transformational activity, which principally occurs via down-wasting (e.g.
353 Fig. 5). An implication of this study is that the ice-cored moraines formed
354 at Austre Lovénbreen, and potentially other valley glaciers in Svalbard (e.g.
355 the recent results of Ewertowski and Tomczyk, 2015), may have higher
356 preservation potential than previously recognised as insulating debris is not
357 reworked and remains *in situ*.

358 During the final stage of moraine development, two end-points are
359 envisaged: (1) a fully stabilised ice-cored moraine, which is in equilibrium
360 with its environment; or (2) an ice-free lateral-frontal moraine complex (Fig.
361 6). The first scenario requires a thick debris mantle to develop that exceeds
362 the permafrost active layer allowing buried-ice to be a persistent landscape
363 feature. It is unclear whether the first scenario is plausible. Ice-cored
364 'controlled' moraines are understood to be poorly preserved in the
365 geomorphological record (Evans, 2009). Buried-ice up to 200 years of age
366 has been documented in moraines at the margins of temperate Icelandic

367 glaciers (e.g. Everest and Bradwell, 2003). Examples of where the
368 preservation of buried-ice has been permitted on longer timescales include
369 formerly glaciated continental settings (e.g. Ingólfsson and Lokrantz, 2003;
370 Murton et al., 2005), and cold deserts where buried-ice is suggested to
371 have existed for several millennia under permafrost conditions (Sugden et
372 al., 1995; Schäfer et al. 2000). Waller et al. (2012) highlighted that the
373 preservation of buried-ice may be permitted on geological timescales if it
374 is located at depths unaffected by seasonal thaw. However, the high-Arctic
375 glacial environment in Svalbard is known for its highly unstable ice-cored
376 moraine, and rapidly progressing mass wasting processes (Bennett et al.,
377 2000; Schomacker, 2008; Irvine-Fynn et al., 2011; Ewertowski and
378 Tomczyk, 2015). Schomacker (2008) showed that climatic variables are
379 only weakly correlated with rates of ice-cored back-wastage occurring at
380 14 different glaciers; the implication being that surface processes and
381 topography are more important determinates of moraine disintegration.
382 However, this result may not hold at Austre Lovénbreen, where very limited
383 evidence of back-wasting was observed in the field by the authors in 1999,
384 2009 and 2014 (e.g. Fig. 5).

385 Alternatively, the second end-point requires complete de-icing of the
386 moraine, where the active layer may continue to exceed the depth of the
387 debris mantle for the duration of the secondary deglaciation process
388 resulting in continued and complete melting of buried-ice despite an
389 increasing debris thickness. The findings of Midgley et al. (2013) indicated
390 that sediment concentration within the moraine is low in lateral positions

391 compared to frontal positions. As a result, following complete de-icing the
392 lateral features which have a significant ice component are likely to be
393 topographically low and diffuse relative to the frontal features where the
394 total volume of sediment appears to be much larger. This is an important
395 consideration where high-Arctic polythermal glaciers are used as an
396 analogue for relict glacial landsystems in the geomorphological record.

397 *5.3. Controls on rates of down-wasting*

398 The physical properties of the insulating debris layer such as its thickness,
399 water content and thermal conductivity influence rates of moraine down-
400 wastage (Schomacker, 2008). The importance of rainwater depends on the
401 extent to which the influence of heat advection via percolation is countered
402 by evaporation from the ground surface (Sakai et al., 2004). Rainwater has
403 been shown to be important in facilitating top-melt in highly permeable
404 substrates (Reznichenko et al., 2010), at least where cool and damp
405 atmospheric conditions limit evaporation. Conversely, block-rich material
406 with high surface roughness has low thermal conductivity and can obstruct
407 the development of winter snow-cover depressing the lower limit of
408 permafrost in mountain terrain (Etzelmüller and Frauenfelder, 2009). At
409 Austre Lovénbreen, the substrate typically consists of clast-rich diamictons
410 which are overlain by gravels with a variable fine component in many places.
411 Diamictons have been associated with variable porosity values (e.g.
412 Parriaux and Nicoud, 1990; Kilfeather and van der Meer, 2008; Burki et al.,
413 2010; Worni et al., 2012). Diamicton with silt and clay components and

414 frozen horizons will lower the permeability of the debris, and serve to
415 impede heat advection by water during summer months, thus limiting ice-
416 ablation (e.g. Reznichenko et al., 2010).

417 Local topographic controls also influence air-temperature and subsequently
418 permafrost distribution (Harris et al. 2009). Strong topographic shading
419 has been reported as an influence on de-icing at other sites in Svalbard
420 (e.g. Lyså and Lønne , 2001). Given the proximity of the landform to
421 Slattofljettet (582 m), rates of moraine down-wastage in up-glacier
422 sections of the landform may be influenced. Modelling of these shading
423 effects is likely to be an interesting avenue of research in relation to
424 moraine disintegration and more generally, permafrost distribution and
425 properties in mountainous terrain.

426 A further confounding factor is snow-cover which is known to limit the
427 influence of atmospheric heat on ground temperature (Stieglitz et al.,
428 2003). Whilst in winter snow may permit higher ground temperature in
429 relation to mean air temperatures (Stieglitz et al., 2003), late lying snow is
430 likely to play an additional role limiting the susceptibility of buried-ice to
431 surface warming. Further work investigating the influence of snow cover
432 and snow-depth in relation to moraine down-wastage could elucidate how
433 significant a role it plays in reducing down-wastage.

434 *5.4. Spatial variations within the moraine system*

435 Diminishing rates of landform change from areas Z_1 to Z_3 (Fig. 3)
436 correspond with an increase in the proportion of debris relative to ice from

437 lateral to frontal positions (e.g. Midgley et al., 2013). Spatially variable
438 amounts of buried-ice imply that the mode of moraine formation is not
439 consistent across the moraine complex (e.g. Hambrey and Glasser, 2012).
440 Lateral sections conform to the 'controlled' ice-cored model of moraine
441 formation (e.g. Evans, 2009) where the release of material from debris-
442 rich folia result in surface linearity and form an insulating surface layer for
443 underlying glacier-ice. The reduced rates of observed surface lowering in
444 the frontal sections, and the presence of surface hummocks indicate that
445 separate glaciological and geomorphological processes are responsible for
446 the emplacement of moraine at different locations along the lateral-frontal
447 complex. Here, structural glaciology and the preferential entrainment of
448 basal debris in frontal locations are likely to be important. For example,
449 studies have investigated the development of surface hummocks
450 ('hummocky moraine') in relation to the stacking of englacial material along
451 thrusts planes (e.g. Hambrey et al., 1996; 1997; Bennett et al., 1998;
452 Graham, 2002; Midgley et al., 2007). The processes described in these
453 papers may, in part, be responsible for areas of surface hummocks on the
454 moraine complex and lower levels of ice incorporation. It is worth noting
455 that additional moraine forming processes such as pushing and permafrost
456 deformation are documented to occur in ice-marginal environments in
457 Svalbard (Etzel Müller et al., 1996; Boulton et al., 1999).

458 6. Summary

459 The evolution of an ice cored lateral-frontal moraine over an 11-year period
460 was assessed at the high-Arctic polythermal glacier Austre Lovénbreen,
461 Svalbard. Repeat DEMs and DEMs of difference were generated from
462 archive and UAV-derived aerial imagery using SfM and minLOD methods.
463 Average depth of surface lowering for the entire study area was estimated
464 to be -1.75 ± 0.89 m. Landform evolution occurred most rapidly on lateral
465 sections of the landform. In contrast to many other sites in Svalbard, field
466 evidence highlights that the moraine appears to be de-icing predominately
467 by down-wastage, affording the landform higher levels of stability. Atypical
468 of de-icing moraines in the high-Arctic, slope and fluvial driven change
469 appear to be less significant. There may be potential for the buried-ice to
470 be stabilised and preserved as a palaeoglaciological archive of former
471 Neoglacial ice dynamics. The high-resolution UAV-derived dataset serves
472 as a benchmark for future studies monitoring geomorphological change on
473 the lateral-frontal moraine at Austre Lovénbreen, achieving a vertical *RMSE*
474 value of 0.048 m for independent check points. This study adds to the
475 growing body of evidence that a combination of UAV-derived imagery, a
476 consumer-grade digital camera and SfM methods are highly appropriate for
477 monitoring of geomorphological change. The errors associated with DEM
478 generation from archived conventional aerial imagery were substantially
479 larger, partly as a result of the lower image resolution, and partly the
480 limited availability of appropriate features to use for ground control. Such
481 issues are common to the extraction of topographic data from archive

482 imagery in changing environments, and may limit the application of this
483 approach. Nevertheless, the derived DEM was of sufficient quality to be
484 useful for estimating the rate of de-icing over the 11-year period
485 investigated. It is concluded that the use of SfM photogrammetry for
486 extracting morphological data from a range of aerial imagery is appropriate
487 for monitoring environmental change and is likely to have wider
488 applications in other geoscientific sub-disciplines.

489 **Acknowledgments**

490 This research was undertaken whilst TNT was funded by a Nottingham Trent
491 University VC bursary. Additional grants from Nottingham Trent University
492 to NGM and from the Manchester Geographical Society to SJC made this
493 work possible. The fieldwork benefited from the logistical support provided
494 by Nick Cox of the UK Natural Environment Research Council (NERC) Arctic
495 Research Station. Anya Wicikowski is thanked for assisting with field data
496 collection. Aerial image data from the UK Natural Environment Research
497 Council (NERC) Airborne Research and Survey Facility (ARSF) are provided
498 courtesy of NERC via the NERC Earth Observation Data Centre (NEODC).
499 Permission to conduct aerial survey work was obtained from the Norwegian
500 CAA and the relevant local authorities. Dr. David Rippin is thanked for
501 providing advice on Norwegian airspace permission applications. Additional
502 thanks go to Marc Shallbrook for providing advice on data preparation. The
503 manuscript was improved following helpful comments from Dr. Marek
504 Ewertowski and one anonymous reviewer.

505 **Fig. 1.** Location map of Svalbard and the study site in relation to Austre
506 Lovénbreen (AL). Data from Norwegian Polar Institute (2014).

507 **Fig. 2.** Locations of ground-control applied to the 2003 and 2014
508 topographic datasets and the independent check-points used for error
509 analysis on the 2014 DEM. The black line indicates the extent of the 2003
510 SfM DEM. The orthophoto is produced from aerial image data collected in
511 2003 by the UK Natural Environment Research Council (NERC) Airborne
512 Research and Survey Facility (ARSF). These data are provided courtesy of
513 NERC via the NERC Earth Observation Data Centre (NEODC).

514 **Fig. 3.** Surface change over the western lateral-frontal moraine of Austre
515 Lovénbreen. (A) DEM of difference for 2003–2014. The black lines are
516 contour data (m.a.s.l.) derived from the 2014 DEM. The locations of three
517 zones of analysis (Z_1 , Z_2 and Z_3) are shown. (B) Surface change in relation
518 to area and volume. (C) Average surface change for Z_1 , Z_2 and Z_3 with the
519 minimum level of detection (minLOD) highlighted by the dotted line.

520 **Fig. 4.** Surface evolution over the 11-year study period demonstrated by
521 three topographic profiles. (A) The locations of the three profiles. (B)
522 Surface change along profiles 1-3 between 2003 and 2014.

523 **Fig. 5.** Relative abundance of geomorphological features indicative of
524 surface change across the study area.

525 **Fig. 6.** Conceptual model for the evolution of the lateral-frontal moraine
526 under the scenarios of partial and complete de-icing.

527 **References**

- 528 Arnold N.S., Rees. W.G., Devereux, B.J. and Amable., G.S. 2006.
529 Evaluating the potential of high-resolution airborne LiDAR data in glaciology.
530 International Journal of Remote Sensing, 27 (6), 1233–1251.
531 doi:10.1080/01431160500353817
- 532 Benn, D.I., Lukas, S., 2006. Younger Dryas glacial landsystems in North
533 West Scotland: An assessment of modern analogues and palaeoclimatic
534 implications. Quaternary Science Reviews. 25, 2390-2408.
535 doi:10.1016/j.quascirev.2006.02.015
- 536 Bennett, G.L. & Evans, D.J.A. 2012. Glacier retreat and landform production
537 on an overdeepened glacier foreland: the debris-charged glacial
538 landsystem at Kvíárjökull, Iceland. Earth Surface Processes and Landforms,
539 37 (15), 1584-1602. doi: 10.1002/esp.3259
- 540 Bennett, M.R., Huddart, D., Hambrey, M.J. and Ghienne, J.F. 1996. Moraine
541 Development at the High-Arctic Valley Glacier Pedersenbreen, Svalbard.
542 *Geografiska Annaler. Series A, Physical Geography*, 78 (4), 209-222.
- 543 Bennett, M.R., Hambrey, M.J., Huddart, D. and Glasser, N.F., 1998. Glacial
544 thrusting and moraine-mound formation in Svalbard and Britain: the
545 example of Coire a' Cheud-chnoic (Valley of hundred hills), Torridon,
546 Scotland. Quaternary Proceedings, 6, 17–34.
- 547 Bennett, M.R., Huddart, D., Glasser, N.F. and Hambrey, M.J. 2000.
548 Resedimentation of debris on an ice-cored lateral moraine in the high-Arctic

549 (Kongsvegen, Svalbard). *Geomorphology*, 35, 21-40. doi:10.1016/S0169-
550 555X(00)00017-9

551 Boulton, G., van der Meer, J.J.M., Beets, D.J., Hart, J.K. and Ruegg, G.H.J.
552 1999. The sedimentary and structural evolution of a recent push moraine
553 complex: Holmstrombreen, Spitsbergen. *Quaternary Science Reviews*, 18,
554 339-371.

555 doi:10.1016/S0277-3791(98)00068-7

556 Brasington, J., Langham, J. and Rumsby B. 2003. Methodological sensitivity
557 of morphometric estimates of coarse fluvial sediment transport.
558 *Geomorphology*, 53 (3–4), 299–316. doi: 10.1016/S0169-555X(02)00320-
559 3

560 Burki, V., Hansen, L., Fredin, O., Andersen, T.A., Beylich, A.A., Jaboyedoff,
561 M., Larsen, E., Tønnesen, J.-F. 2010. Little Ice Age advance and retreat
562 sediment budgets for an outlet glacier in western Norway. *Boreas*, 39 (3)
563 (2010), 551–566. doi: 10.1111/j.1502-3885.2009.00133.x

564 Clapuyt, F., Vanacker, V., Van Oost, K. 2015. Reproducibility of uav-based
565 earth topography reconstructions based on structure-from-motion
566 algorithms. *Geomorphology*, In press.
567 doi:10.1016/j.geomorph.2015.05.011

568 Carrivick, J.L., Smith, M.W., Quincey, D.J. and Carver, S.J. 2013.
569 Developments in budget remote sensing for the geosciences. *Geology*
570 Today, 29, 138–143. doi: 10.1111/gto.12015

571 Etzelmüller, B. 2000. Quantification of thermo-erosion in pro-glacial areas
572 - examples from Svalbard. *Zeitschrift für Geomorphologie*, 44, 343-361.

573 Etzelmüller, B. and Frauenfelder, R. 2009. Factors Controlling The
574 Distribution of Mountain Permafrost in The Northern Hemisphere and Their
575 Influence on Sediment Transfer. *Arctic, Antarctic, and Alpine Research*, 41
576 (1), 48-58. DOI: 10.1657/1938-4246(08-026)[ETZELMUELLER]2.0.CO;2

577 Etzelmüller, B. and Hagen, J.O. 2005. Glacier permafrost interaction in
578 arctic and alpine environments – examples from southern Norway and
579 Svalbard. In: Harris, C. & Murton, J. (eds.). *Cryospheric systems – Glaciers
580 and Permafrost*. British Geol. Soc., Spec. Publ. 242, 11-27.

581 Etzelmüller, B., Hagen, J.O., Vatne, G., Ødegård, R.S., Sollid, J.L. 1996.
582 Glacier debris accumulation and sediment deformation influenced by
583 permafrost, examples from Svalbard. *Ann. Glaciol.*, 22, 53 – 62.

584 Etzelmüller, B., Ødegård, R.S., Vatne, G., Mysterud, S., Tonning, T and
585 Sollid, J.L. 2000. Glacier characteristics and sediment transfer system of
586 Longyearbreen and Larsbreen, western Spitsbergen. *Norsk Geografisk
587 Tidsskrift*, 54 (4), 157-168. DOI:10.1080/002919500448530

588 Evans, D.J.A. 2009. Controlled moraines: origins, characteristics and
589 palaeoglaciological implications. *Quaternary Science Reviews*, 28 (3-4),
590 181-260. doi: 10.1016/j.quascirev.2008.10.024

591 Everest, J. and Bradwell, T. 2003. Buried glacier ice in southern Iceland and
592 its wider significance. *Geomorphology*, 52 (3-4). 347–358.
593 [http://dx.doi.org/10.1016/S0169-555X\(02\)00277-5](http://dx.doi.org/10.1016/S0169-555X(02)00277-5)

594 Ewertowski M., Kasprzak L., Szuman I., Tomczyk A.M., 2012. Controlled,
595 ice-cored moraines: sediments and geomorphology. An example from
596 Ragnarbreen, Svalbard. *Zeitschrift für Geomorphologie*, 56 (1), 53-74. doi:
597 10.1127/0372-8854/2011/0049

598 Ewertowski. M. 2014. Recent transformations in the high-Arctic glacier
599 landsystem, Ragnarbreen, Svalbard. *Geografiska Annaler: Series A*
600 *(Physical Geography)*, 96, 265-285. doi: 10.1111/geoa.12049

601 Ewertowski, M. and Tomczyk, A.M. 2015. Quantification of the ice-cored
602 moraines' short-term dynamics in the high-Arctic glaciers Ebbabreen and
603 Ragnarbreen, Petuniabukta, Svalbard. *Geomorphology*, 234, 211-227. doi:
604 10.1016/j.geomorph.2015.01.023

605 Friedt, J.-M., Tolle, F., Bernard, É., Griselin, M., Laffy, D and Marlin, C. 2012.
606 Assessing the relevance of digital elevation models to evaluate glacier mass
607 balance: application to Austre Lovénbreen (Spitsbergen, 79°N). *Polar*
608 *Record*, 48 (244) 2–10. DOI: 10.1017/S0032247411000465

609 Fonstad, M.A., Dietrich, J.T., Courville, B.C. and Carbonneau, P.E. 2013.
610 Topographic structure from motion: a new development in
611 photogrammetric measurements. *Earth Surface Processes and Landforms*,
612 20, 817-827. doi: 10.1002/esp.3366

613 Graham, D.J. 2002. Moraine–mound formation during the Younger Dryas
614 in Britain and the Neoglacial in Svalbard. PhD thesis University of Wales,
615 Aberystwyth.

616 Graham, D.J. and Hambrey, M.J. 2007. Sediments and landforms in an
617 upland glaciated-valley landsystem: Upper Ennerdale, English Lake District
618 in M.J. Hambrey, P. Christoffersen, N.F. Glasser NF and B. Hubbard (Eds),
619 Glacial Sedimentary Processes and Products, Blackwell, Oxford (2007),
620 235-256.

621 Graham, D.J. and Midgley, N.G. 2000. Moraine-mound formation by
622 englacial thrusting: the Younger Dryas moraines of Cwm Idwal, North
623 Wales. In: A.J. Maltman, B. Hubbard and M.J. Hambrey (eds.), Deformation
624 of Glacial Materials. London: Geological Society, pp. 321-336.
625 <http://dx.doi.org/10.1144/GSL.SP.2000.176.01.24>

626 Glasser, N.F. and Hambrey, M.J. 2003. Ice-marginal terrestrial landsystems:
627 Svalbard polythermal glaciers in D.J.A. Evans (Ed.), Glacial Landsystems,
628 Hodder Arnold, London (2003), 65–88.

629 Glasser, N.F., Coulsen, S.J., Hodkinson, I.D. and Webb, N.R. 2004.
630 Photographic evidence of the return period of a Svalbard surge-type glacier:
631 a tributary of Pedersenbreen, Kongsfjord. *Journal of Glaciology*, 50 (169),
632 307-308.

633 Hambrey, M.J., Dowdeswell, J.A., Murray, T., Porter, P.R., 1996. Thrusting
634 and debris entrainment in a surging glacier: Bakaninbreen, Svalbard.
635 *Annals of Glaciology*, 22, 241-248.

636 Hambrey, M.J., Huddart, D., Bennett, M.R. and Glasser, N.F. 1997. Genesis
637 of "hummocky moraines" by thrusting in glacier ice: evidence from
638 Svalbard and Britain. *Journal of the Geological Society, London*. 154, 623-
639 632. doi: 10.1144/gsjgs.154.4.0623

640 Hambrey, M.J., Murrery, T., Glasser, N.F., Hubbard, A., Hubbard, B., Stuart,
641 G., Hansen, S. and Kohler, J. 2005. Structure and changing dynamics of a
642 polythermal valley glacier on a centennial time-scale: midre Lovénbreen,
643 Svalbard. *Journal of Geophysical Research, Earth Surface*, p. F010006.

644 Hambrey, M.J. and Glasser, N.F. 2012. Discriminating glacier thermal and
645 dynamic regimes in the sedimentary record, *Sedimentary Geology*, 251–
646 252, 1–33. doi:10.1016/j.sedgeo.2012.01.008

647 Hansen, S. 2003. From surge-type to non-surge type glacier behaviour:
648 Midre Lovénbreen, Svalbard. *Annals of Glaciology*, 36, 97–102.

649 Harris, C., Arenson, L.U., Christiansen, H.H., Etzelmüller, B., Fraunfelder,
650 R., Gruber., Haeberli, W., Hauck, C., Hölzle, M., Humlum, O., Isaksen, K.
651 Käab, A., Kern-Lütschg, M.A., Lehning, M., Matsuoka, N., Murton, J.B.,
652 Nötzlie, J., Philips, M., Ross, N., Seppäläl, M., Springman, S.M. and Mühl,
653 D.V. 2009. Permafrost and climate in Europe: Monitoring and modelling
654 thermal, geomorphological and geotechnical responses. 92 (3-4), 117-171.
655 doi: 10.1016/j.earscirev.2008.12.002

656 Isachsen, G. 1912. *Exploration du Nord-Ouest du Spitsberg entreprise sous*
657 *les auspices de S.A.S. le Prince de Monaco par la Mission Isachsen.*
658 *Fascicule XL. Imprimerie de Monaco.*

659 Irvine-Fynn, T.D.L., Barrand, N.E., Porter, P.R., Hodson, A.J. and Murray,
660 T. 2011. Recent High-Arctic glacial sediment redistribution: a process
661 perspective using airborne lidar. *Geomorphology*, 125 (1), 27–39.
662 doi:10.1016/j.geomorph.2010.08.012

663 Ingólfsson, Ó and Lokrantz, H. 2003. Massive ground ice body of glacial
664 origin at Yugorski Peninsula, arctic Russia. *Permafrost and Periglacial*
665 *Processes*, 14 (3), 199–215. doi: 10.1002/ppp.455

666 James, M. R. and Robson, S. 2012. Straightforward reconstruction of 3D
667 surfaces and topography with a camera: Accuracy and geoscience
668 application, *J. Geophys. Res.*, 117, F03017, doi: 10.1029/2011JF002289

669 Jiskoot, H., Murray, T. and Boyle, P.J. 2000. Controls on the distribution of
670 surge-type glaciers in Svalbard. *Journal of Glaciology*, 46 (154) 412–422.
671 doi: 10.3189/172756500781833115

672 King, E.C., Smith, A.M., Murray, T. and Stuart, G.W. 2008. Glacier-bed
673 characteristics of midtre Lovénbreen, Svalbard, from high - resolution
674 seismic and radar surveying, *J. Glaciol.*, 54, 145 - 156,
675 doi:10.3189/002214308784409099.

676 Kilfeather , A.A. and van der Meer, J.J.M. 2008. Pore size, shape and
677 connectivity in tills and their relationship to deformation processes.
678 *Quaternary Science Reviews*, 27 (3–4) 250–266. doi:
679 10.1016/j.quascirev.2006.12.015

680 Kirkbride, M.P. and Winkler, S. 2012. Correlation of Late Quaternary
681 moraines: impact of climate variability, glacier response, and chronological
682 resolution. *Quaternary Science Reviews*, 46, 1-29.
683 doi:10.1016/j.quascirev.2012.04.002

684 Kjær, K.H and Krüger, J. 2001. The final phase of dead-ice moraine
685 development: processes and sediment architecture, Kötlujökull, Iceland.
686 *Sedimentology*, 48 (5), 935-952. doi: 10.1046/j.1365-3091.2001.00402.x

687 Krüger, J. and Kjær, K.H. 2000. De-icing progression of ice-cored moraines
688 in a humid, sub-polar climate, Kötlujökull, Iceland. *The Holocene*, 48, 935–
689 952. doi: 10.1191/09596830094980

690 Krüger, J., Kjær, K.H., Schomacker, A. 2010. Dead-Ice Environments: A
691 Landsystems Model for a Debris-Charged, Stagnant Lowland Glacier Margin,
692 Kötlujökull. *Developments in Quaternary Sciences*. 13, 105-126.
693 doi:10.1016/S1571-0866(09)01307-4

694 Lønne, I. and Lyså, A. 2005. Deglaciation dynamics following the Little Ice
695 Age on Svalbard: Implications for shaping of landscapes at high latitudes.
696 *Geomorphology* 72, 300–319. doi:10.1016/j.geomorph.2005.06.003

697 Lucieer, A., de Jong, S.M, and Turner, D. 2013. Mapping landslide
698 displacements using Structure from Motion (SfM) and image correlation of
699 multi-temporal UAV photography. *Progress in Physical Geography*, 38 (1),
700 97-116. doi: 10.1177/0309133313515293

701 Lukas, S., Nicholson, L.I., Ross, F.H and Humlum, O. 2005 Formation,
702 meltout processes and landscape alteration of High-Arctic ice-cored
703 moraines—examples from Nordenskiöld Land, Central Spitsbergen. *Polar*
704 *Geography*, 29 (3), 157–187. doi: 10.1080/789610198

705 Lyså, A. and Lønne. I. 2001. Moraine development at a small High-Arctic
706 valley glacier: Rieperbreen, Svalbard. *Journal of Quaternary Science*, 16
707 (6), 519–529. doi: 10.1002/jqs.613

708 Midgley, N.G., Glasser, N.F. and Hambrey, M.J. 2007. Sedimentology,
709 structural characteristics and morphology of a Neoglacial high-Arctic
710 moraine–mound complex: Midre Lovénbreen, Svalbard. in: M.J. Hambrey,
711 P. Christoffersen, N.F. Glasser, B. Hubbard (Eds.), *Glacial Sedimentary*
712 *Processes and Products*, International Association of Sedimentologists,
713 *Special Publication*, 39 (2007), 11–23.

714 Midgley, N.G., Cook, S.J., Graham, D.J. and Tonkin, T.N. 2013. Origin,
715 evolution and dynamic context of a Neoglacial lateral–frontal moraine at
716 Austre Lovénbreen, Svalbard. *Geomorphology*, 198, 96–106.
717 doi:10.1016/j.geomorph.2013.05.017

718 Murton J.B., Whiteman, C.A., Waller, R.I., Pollard, W.H., Clark, I.D. and
719 Dallimore, S.R. 2005. Basal ice facies and supraglacial melt-out till of the
720 Laurentide Ice Sheet, Tuktoyaktuk Coastlands, western Arctic Canada.
721 *Quaternary Science Reviews*. 24 (5-6), 681–708.
722 doi: 10.1016/j.quascirev.2004.06.008

723 Norwegian Polar Institute 2014. Kartdata Svalbard 1:100 000 (S100
724 Kartdata). Tromsø, Norway: Norwegian Polar Institute. Available at:
725 <https://data.npolar.no/dataset/645336c7-adfe-4d5a-978d-9426fe788ee3>

726 Parriaux, A. and Nicoud, G.F. 1990. Hydrological behaviour of glacial
727 deposits in mountainous areas, in: L. Molnár (Ed.), *Hydrology of*
728 *Mountainous Areas*, International Association of Hydrological Sciences,
729 Publication, 190 (1990), 291–311.

730 Reznichenko, N., Davies, T., Shulmeister, J. and McSaveney, M. 2010.
731 Effects of debris on ice surface melting rates: an experimental study.
732 *Journal of Glaciology*, 56 (197), 384-394. doi:
733 10.3189/002214310792447725

734 Rippin, D.M., Pomfret, A. and King, N. 2015. High resolution mapping of
735 supra-glacial drainage pathways reveals link between micro-channel
736 drainage density, surface roughness and surface reflectance. *Earth Surface*
737 *Processes and Landforms*. Early view. doi: 10.1002/esp.3719

738 Ryan, J.C., Hubbard, A.L., Box, J.E., Todd, J., Christoffersen, P., Carr, J.R.,
739 Holt, T.O., Snooke, N. 2015. UAV photogrammetry and structure from
740 motion to assess calving dynamics at Store Glacier, a large outlet draining
741 the Greenland ice sheet. *The Cryosphere*, 9, 1-11. doi:10.5194/tc-9-1-
742 2015

743 Sakai, A., Fujita, K. and Kubota, J. 2004. Evaporation and percolation effect
744 on melting at debris-covered Lirung Glacier, Nepal Himalayas, 1996.
745 *Bulletin of Glaciological Research*, 21, 9–16.

746 Saintenoy, A., Friedt, J.-M., Booth, A.D., Tolle, F., Bernard, E., Laffly, D.,
747 Marlin, C. and Griselin, M. 2012. Deriving ice thickness, glacier volume and
748 bedrock morphology of Austre Lovénbreen (Svalbard) using GPR. *Near*
749 *Surface Geophysics*, 11 (2), 253–26. doi: 10.3997/1873-0604.2012040

750 Schäfer, J.M., Heinrich, B., Denton, G.H., Ivy-Ochs, S., Marchant, D.R.,
751 Schlüchter, C. and Rainer, W. 2000. The oldest ice on Earth in Beacon
752 Valley, Antarctica: new evidence from surface exposure dating. *Earth and*
753 *Planetary Science Letters*. 179 (1), 91-99.

754 Schiefer, E. and Gilbert, R. 2007. Reconstructing morphometric change in
755 a proglacial landscape using historical aerial photography and automated
756 DEM generation. *Geomorphology*, 88 (1-2), 167-178.
757 doi:10.1016/j.geomorph.2006.11.003

758 Schomacker, A. 2008. What controls dead-ice melting under different
759 climate conditions? A discussion. *Earth-Science Reviews*, 90 (3-4), 103-113.

760 Schomacker, A. and Kjær, K.H. 2007. Origin and de-icing of multiple
761 generations of ice-cored moraines at Brúarjökull, Iceland. 36 (4), 411-425.

762 Schomacker, A. and Kjær, K.H. 2008. Quantification of dead-ice melting in
763 ice-cored moraines at the high-Arctic glacier Holmstrombreen, Svalbard.
764 *Boreas*, 37, 211–225. doi: 10.1111/j.1502–3885.2007.00014.x.

765 Smith, M.W. and Vericat, D. 2015. From experimental plots to experimental
766 landscapes: topography, erosion and deposition in sub-humid badlands

767 from Structure-from-Motion photogrammetry. *Earth Surface Processes and*
768 *Landforms*. Early View. doi: 10.1002/esp.3747

769 Staines, K.E., Carrivick, J.L., Tweed, F.S., Evans, A.J., Russell, A.J.,
770 Jóhannesson, T. and Roberts, M. 2015. A multi-dimensional analysis of
771 proglacial landscape change at Sólheimajökull, southern Iceland. *Earth*
772 *Surface Processes and Landforms*. Available online from 14/11/2014. doi:
773 10.1002/esp.3662

774 Stieglitz, M., Déry, S.J., Romanovsky, V.E., Osterkamp, T.E. 2003. The
775 role of snow cover in the warming of arctic permafrost. *Geophysical Research*
776 *Letters*, 30 (13), 1721. doi:10.1029/2003GL017337

777 Sugden, D.E., Marchant, D.R., Potter Jr. N., Souchez, R.A., Denton, G.H.,
778 Swischer III, C.C. and Tison, J.-L. 1995. Preservation of Miocene glacier ice
779 in East Antarctica. *Nature*, 376, 412–414. doi:10.1038/376412a0

780 Tonkin, T.N., Midgley, N.G., Graham, D.J. and Labadz, J.C. 2014. The
781 potential of small unmanned aircraft systems and structure-from-motion
782 for topographic surveys: A test of emerging integrated approaches at Cwm
783 Idwal, North Wales. *Geomorphology*, 226, 35-43. doi:
784 10.1016/j.geomorph.2014.07.021

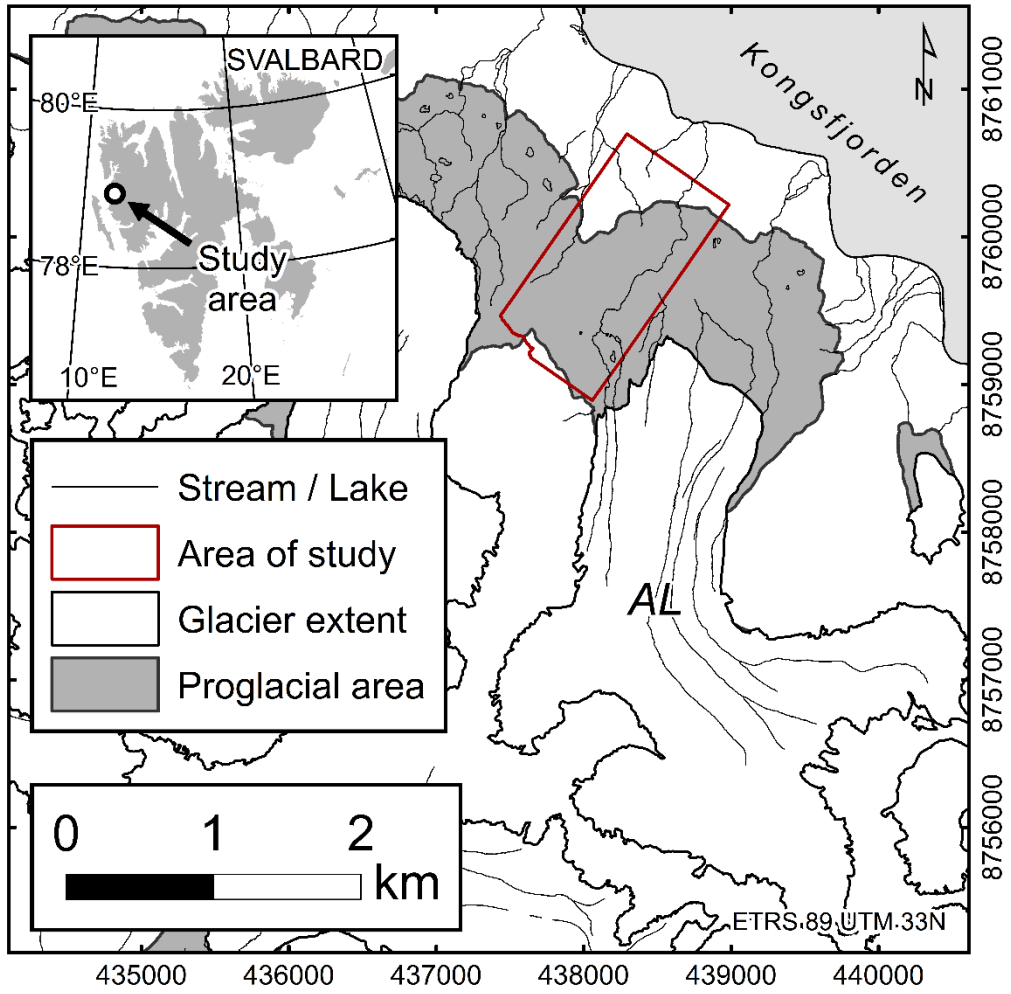
785 Waller, R.I., Murton, J.B. and Kristensen, L. 2012. Glacier-permafrost
786 interactions: Processes, products and glaciological implications.
787 *Sedimentary Geology*, 255, 1-28. doi: /10.1016/j.sedgeo.2012.02.005

788 Wheaton, J.M., Brasington, J., Darby, S.E. and Sear, D.A. 2010. Accounting
789 for uncertainty in DEMs from repeat topographic surveys: improved
790 sediment budgets. *Earth Surface Processes and Landforms*, 35 (2), 136-
791 156. doi: 10.1002/esp.1886

792 Worni, R., Stoffel, M., Huggel, C., Volz, C., Casteller, A. and Luckman, B.
793 2012. Analysis and dynamic modeling of a moraine failure and glacier lake
794 outburst flood at Ventisquero Negro, Patagonian Andes (Argentina). *Journal*
795 *of Hydrology*, 444–445, 134–145. doi:10.1016/j.jhydrol.2012.04.013

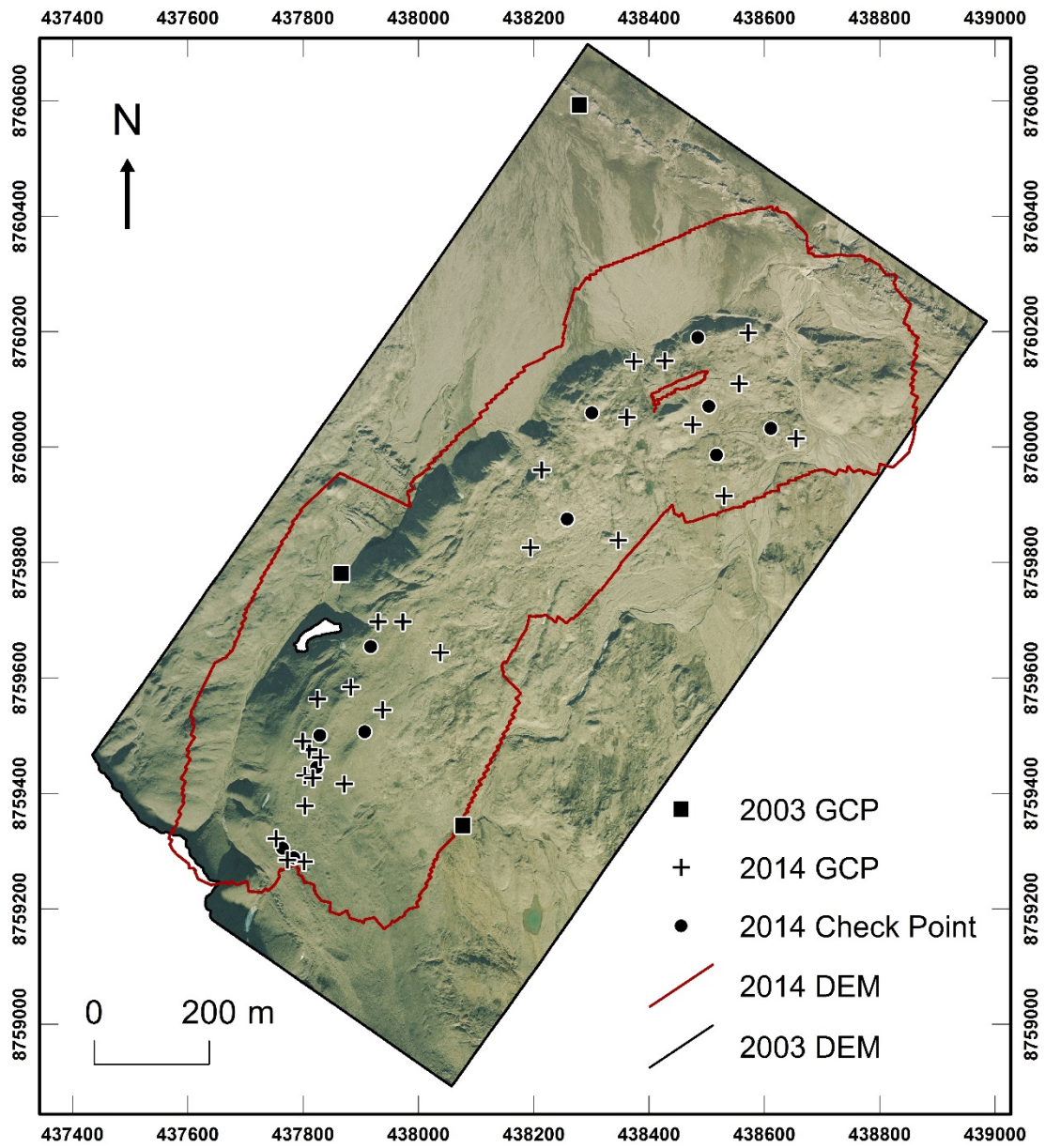
796 Westoby, M., Brasington J, Glasser, N.F., Hambrey, M.J. and Reynolds, M.J.
797 2012. Structure-from-Motion photogrammetry: a low-cost, effective tool
798 for geoscience applications. *Geomorphology*, 179, 300-314.
799 doi:10.1016/j.geomorph.2012.08.021

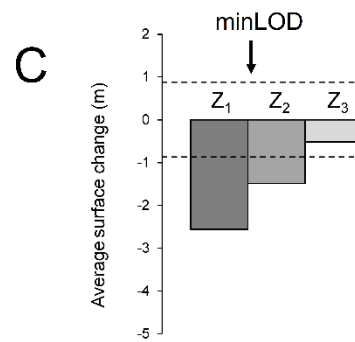
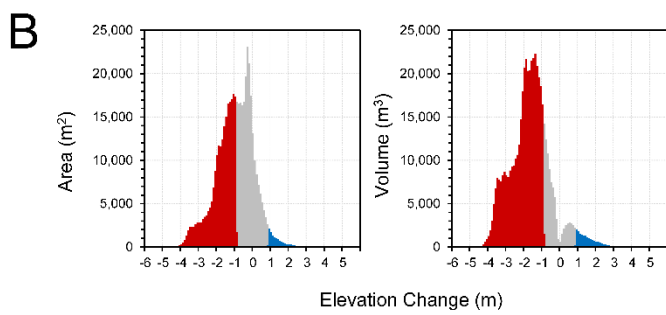
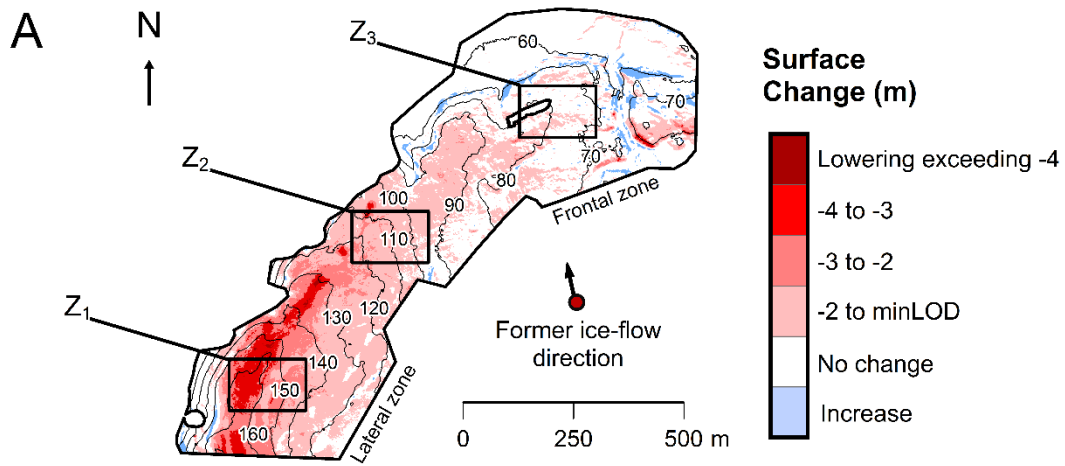
800



801

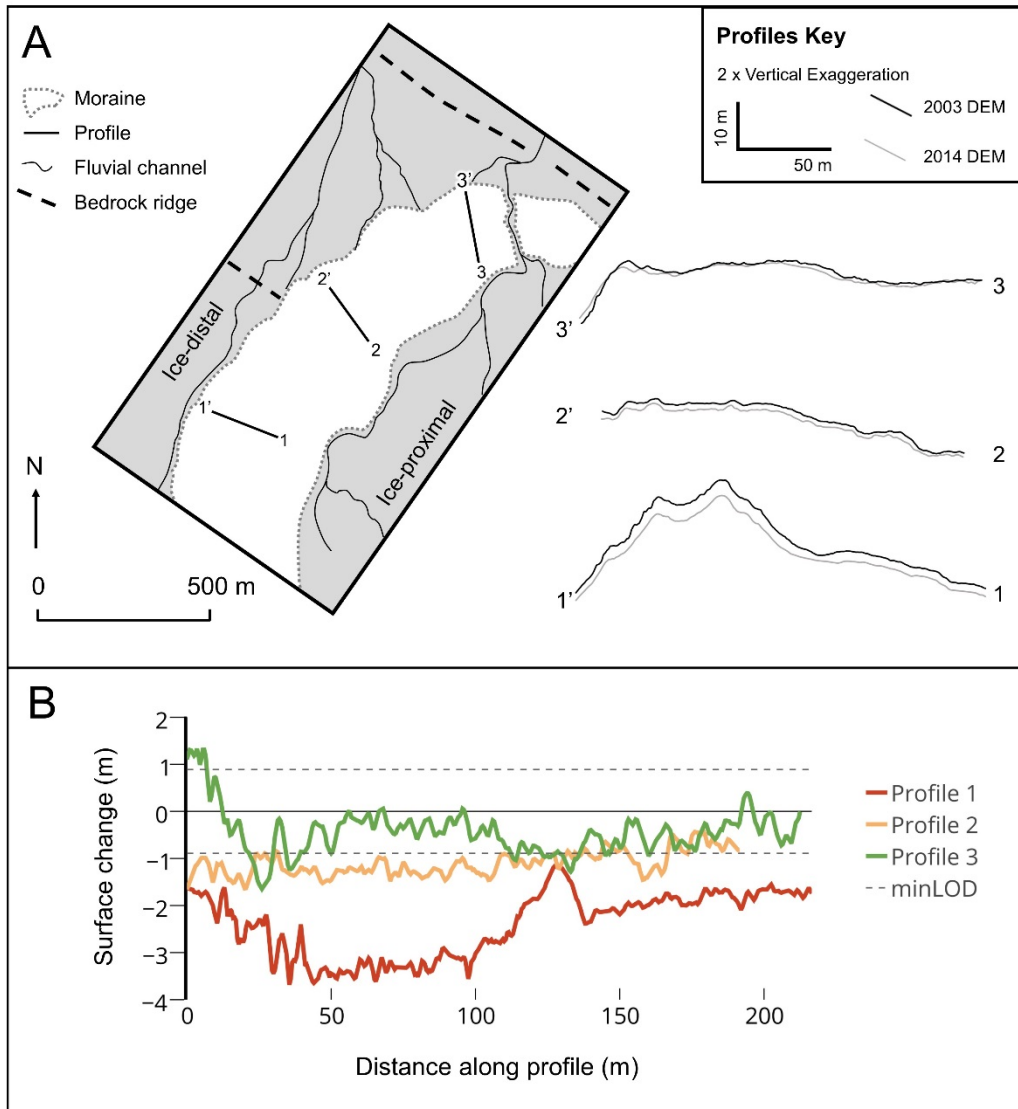


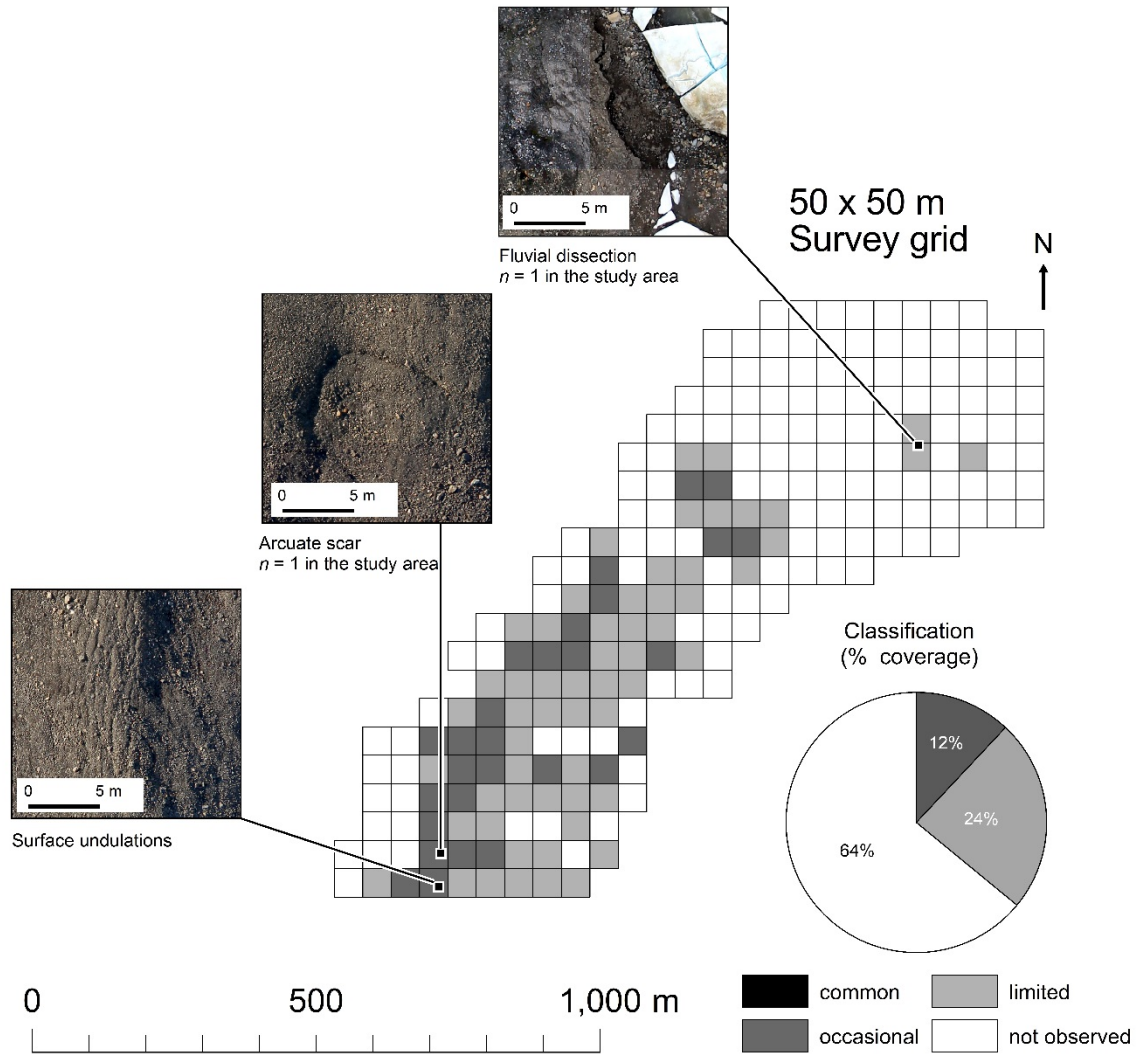




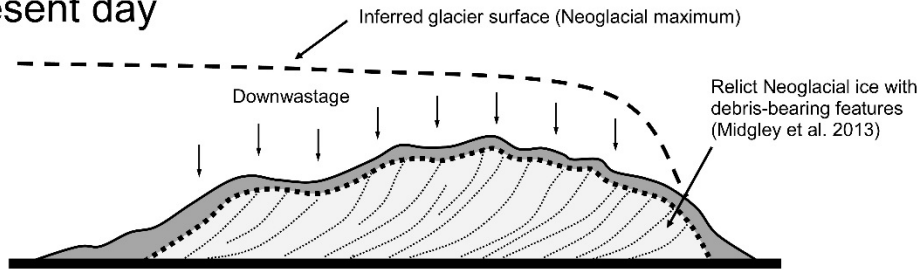
803

DRAFT

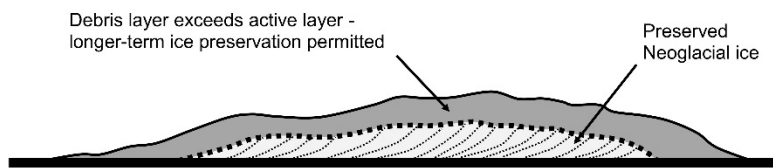




Present day



End-point I: Partial de-icing



End-point II: Complete de-icing

